THE JOURNAL OF PHYSICAL CHEMISTRY C

ARTICLE

pubs.acs.org/JPCC

A Triplet Form of (5,0) Carbon Nanotube with Higher Hydrogen Storage Capacity

Y. W. Wen,[†] H. J. Liu,*[,†] L. Pan,[†] X.J. Tan,[†] H. Y. Lv,[†] J. Shi,[†] and X. F. Tang[‡]

[†]Key Laboratory of Artificial Micro- and Nano-structures of Ministry of Education and School of Physics and Technology, Wuhan University, Wuhan 430072, China

[‡]State Key Laboratory of Advanced Technology for Materials Synthesis and Processing, Wuhan University of Technology, Wuhan 430072, China

ABSTRACT: Using density functional calculations, we study the structural, energetic, and electronic properties of a triplet form of (5,0) carbon nanotube. In contrast to the weak tube−tube interactions found in a bundle of large diameter nanotubes, the ultrasmall (5,0) tubes within the triplet are covalently connected and appear like a three-blade electric fan from a top view. The triplet is energetically most favorable and is the only semiconductor among all the small bundles of (5,0) tubes. Due to its unique atomic configuration, chemisorptions of hydrogen on the triplet show interesting site dependence. When the physisorptions are also included in the system, the hydrogen storage capacity can reach 10.4 wt %.

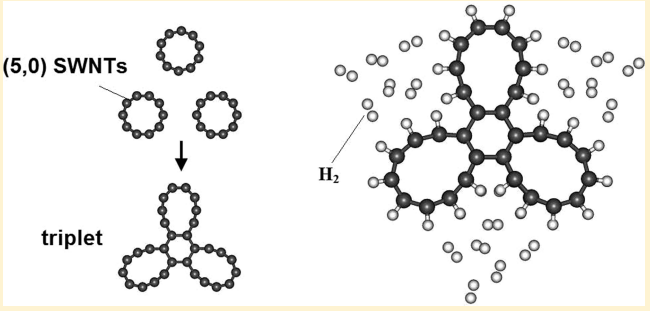

1. INTRODUCTION

Carbon nanotubes observed in the experiments usually self-organize into a crystalline bundle where the tubes are arranged in a two-dimensional hexagonal lattice,[1,2] and a van der Waals (vdW) interaction is generally assumed between them. The bundle exhibits various pore structures including the interior of tube, the interstitial channels between the tubes, and the groove sites separating two adjacent tubes on the outer surface. As a result, a bundle of nanotubes is an ideal candidate for ion intercalation or molecule adsorption and may have potential applications in energy storage,[3−6] gas sensors,[7−9] quantum sieving,[10,11] and isotope separation.[12,13] In addition, superconductivity has been observed in carbon nanotube bundles,[14−16] and the superconducting transition temperature T_c is supposed to be affected by the intertube Josephson coupling.[17]

The tube−tube interactions within a bundle have attracted a lot of attention from the science community.[18−22] Tersoff investigated the vdW interaction in a series of carbon nanotube bundles and found that the tubes with a diameter less than 10 Å will keep rigid cylindrical shape, while those larger than 25 Å will be reshaped into a honeycomb configuration.[18] However, another simulation shows that such weak interaction could be changed into strong chemical bonds in the (10,10) carbon nanotube bundle, and it will be coalesced into a multiwall nanotube under thermal treatment.[20] In this work, we will focus on the (5,0) carbon nanotube which has a diameter of about 4 Å, probably at or close to the theoretical limit. It should be mentioned that there are actually three kinds of 4 Å carbon nanotubes, namely, the zigzag (5,0), the armchair (3,3), and the chiral (4,2), and all of them are known to be fabricated using a template method.[23] While these tubes are usually confined inside the AFI zeolite channels, the AFI can be dissolved by acid to recover them as standalone entities. Due to the large curvature, these ultrasmall nanotubes are expected to be more reactive than larger-diameter ones and might self-organize into crystalline bundles from a well aligned initial geometry. It is thus natural to ask whether such a bundle is stable and what are the tube−tube interactions. We will find from density functional calculations that the (5,0) tubes prefer to form the bundle state by strong chemical bonds rather than the weak vdW interactions. The most energetically favorable product contains three covalently connected (5,0) tubes which appears like a three-blade electric fan from a top view. The electronic properties of such a triplet bundle are compared with those of the freestanding (5,0) tube, and hydrogen adsorptions on the triplet are discussed in detail.

2. COMPUTATIONAL DETAILS

Our density-functional calculations have been performed using the projector-augmented-wave (PAW)[24] method within the framework of local density approximation (LDA). The code is implemented in the Vienna ab initio Simulation Package (VASP).[25−27] We adopt a standard hexagonal supercell with dimensions of 24 Å × 24 Å × 4.22 Å for the bundle structure, and 32 Å × 32 Å × 4.22 Å for the case of hydrogen adsorption. Such large separation allows for negligible interaction between the bundle and its periodic images. The plane-wave cutoff is set to

Received: December 19, 2010
Revised: March 31, 2011
Published: April 15, 2011

dx.doi.org/10.1021/jp1120433 | J. Phys. Chem. C 2011, 115, 9227–9231

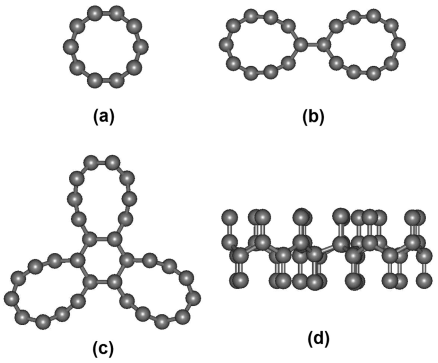

Figure 1. Ball-and-stick model of (a) freestanding (5,0) tube, (b) (5,0) doublet bundle, and (c) (5,0) triplet bundle. (d) Side view of c.

400 eV, and the Brillouin zone of the supercell is sampled with 1 × 1 × 20 Monkhorst meshes. The atomic positions are fully optimized until the magnitude of the forces acting on all atoms become less than 0.05 eV/Å.

3. RESULTS AND DISCUSSION

We begin our investigation with the bundle structure containing only two (5,0) tubes. During the calculations, the initial tube−tube distance is set to 3.4 Å, and their relative orientations are carefully checked to find the minimum energy configuration. The fully relaxed doublet structure is shown in Figure 1b. We see that two (5,0) tubes are joined together with one bridging bond, and the cross-section becomes elliptical compared with the freestanding case (Figure 1a). A similar shape can be found in the triplet bundle where the three (5,0) tubes are covalently connected and appears like a three-blade electric fan from a top view (Figure 1c). It is interesting to find that the center of the (5,0) triplet is actually a (3,0) nanotube with sp^3 hybridization of the carbon atoms (Figure 1d). We have also considered the bundle of four (5,0) tubes and find that the quadruplet product with the lowest energy is composed of a triplet covalently connected by a single (5,0) tube (not shown here). This structure has obviously lower symmetry compared with those of the doublet and triplet.

To investigate the energetic stability of these small bundles, we have calculated the average heat of formation E_h which is defined as:

$$E_h = [E(\text{bundle}) - n \times E(\text{tube})]/n$$

where E(bundle) is the total energy of the bundle consisting of n (5,0) tubes, and E(tube) is the total energy of a freestanding tube. A negative value of E_h indicates stronger binding and higher stability of the system. The calculated E_h for the above-mentioned doublet, triplet, and quadruplet bundles are −1.01 eV, −2.39 eV, and −2.04 eV per unit cell, respectively. Note that the periodicity along the bundle axis is 4.26 Å, and these values correspond to a E_h of −0.24 eV, −0.56 eV, and −0.48 eV per unit length, respectively. We see that all the systems have a negative heat of formation which means that the aggregations of the (5,0) tubes to form small bundles should be energetically favorable. Moreover, the considerably large number of E_h indicates that there are strong tube−tube interactions within a (5,0) bundle. Indeed, these (5,0) tubes are found to be covalently connected as shown in Figure 1. This finding is very different from previous results for most bundles where a weak vdW interaction is responsible for their stability. The reason is probably related to the ultrasmall diameter of the (5,0) tube where the strong curvature makes the tube walls more reactive. To verify this point, we have considered the doublet bundle of (6,0) and (8,0) tubes which have relatively larger diameters. Unlike the (5,0) tube, we find that two (6,0) or (8,0) tubes can be weakly bound at a distance of about 3.2 Å. The calculated E_h (per unit cell) are −0.07 eV and −0.08 eV for the (6,0) and (8,0) doublets, respectively. It should be mentioned that bundle state with strong chemical bonds can be also found for the (6,0) and (8,0) tubes when they get close to each other at a distance of about 1.5 Å. The heat of formation (per unit cell) is −1.03 eV for the (6,0) and −0.35 eV for the (8,0) products. To estimate the energy barriers between the weakly and strongly bound states, eight intermediate images of each system are constructed between them and the corresponding energies are calculated. This approach gives the minimum energy path, and the estimated energy barriers are 0.12 and 0.38 eV for the (6,0) and (8,0) tubes, respectively. In contrast, there is no energy barrier when two (5,0) tubes are put closer to each other and form the strongly bound doublet. This explains why there is no weakly bound state for the (5,0) tubes, and we always obtain the covalently connected bundle. We further find that with the increasing of tube diameter, the energy barriers become larger which only favors the existence of the weakly bound state of the vdW type, as usually mentioned in the literature. It should be noted that we have also done calculations for the (3,3) tube which has almost the same diameter as the (5,0) tube but with quite different chirality. Unlike the (5,0) tube, we find that it is energetically unfavorable to form the (3,3) triplet. The corresponding heat of formation (per unit cell) is 0.35 eV compared with −2.39 eV of the (5,0) triplet. This observation suggests that in addition to the tube diameter, the chirality also plays an important role in the formation of carbon nanotube bundle.

The strong tube−tube interactions within the (5,0) bundle can also be indicated by investigation of the differential charge density contour, which is defined as the difference between the charge density of the bundle and that of the freestanding (5,0) tube. Figure 2 shows the differential charge density contour on the plane perpendicular to the tube axis. We see that for both the doublet and triplet bundles, there are obvious charge accumulations between carbon atoms from neighboring tubes. Again this contour plot confirms the fact that the (5,0) tubes are covalently connected by the sp^3 carbon atoms to form the bundles.

Figure 3 shows the calculated energy band structures of the above-mentioned bundles of (5,0) tubes. The band structure is plotted with 50 uniform **k** points along the tube axis. For comparison, the result for a freestanding (5,0) tube (or singlet) is also shown. As known,[28] a (5,0) tube is metallic due to its strong curvature effect. When two (5,0) tubes are covalently connected, we see from Figure 3b that the doublet is still metallic and those bands near the Fermi level are similar in topology to those of the singlet (see Figure 3a). However, the degenerated bands are now separated due to the elliptical distortion of the (5,0) tubes. In contrast, we see from Figure 3c that the triplet is a semiconductor with an indirect band gap of 0.51 eV caused by strong repulsion between the α and β bands around the Fermi level. We have also calculated the band structure of the quadruplet (not shown here) and find it is also metallic and appears like an overlap of the bands of the singlet and triplet. The distinct semiconducting behavior of the triplet bundle is probably related to more severe deformation of the tubular structure and especially its larger ratio of sp^3 carbon atoms. It was previously found

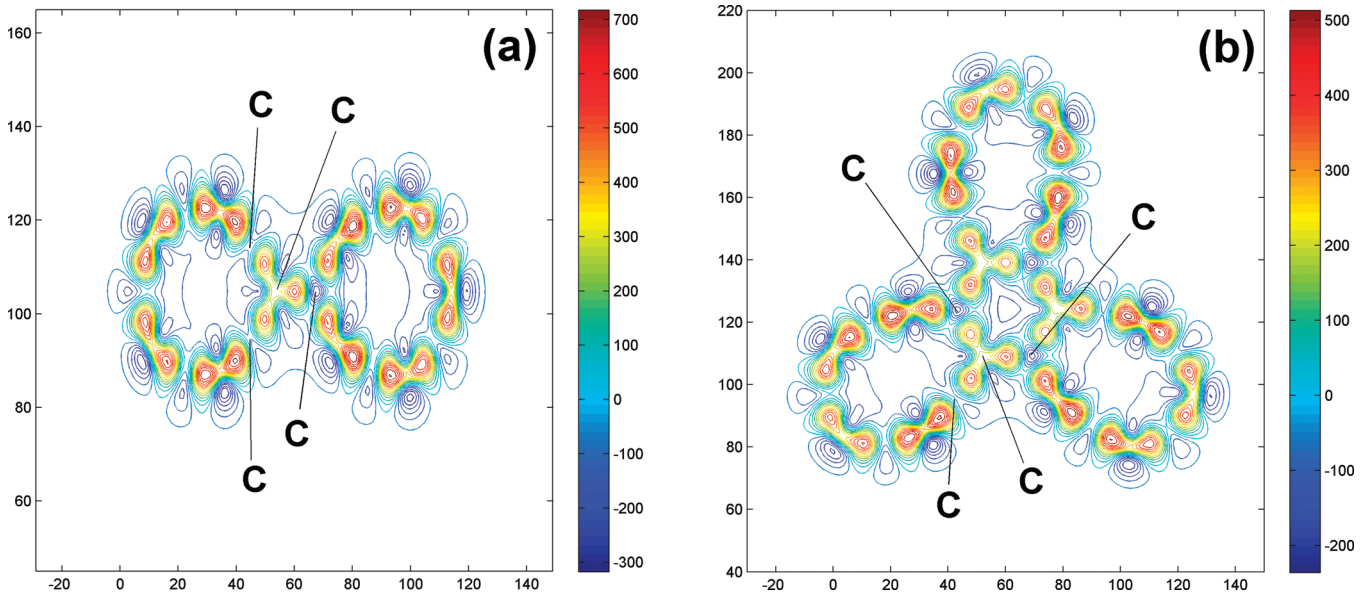

Figure 2. Differential charge density contour plot on the planes perpendicular to the tube axis for (a) (5,0) doublet bundle, and (b) (5,0) triplet bundle.

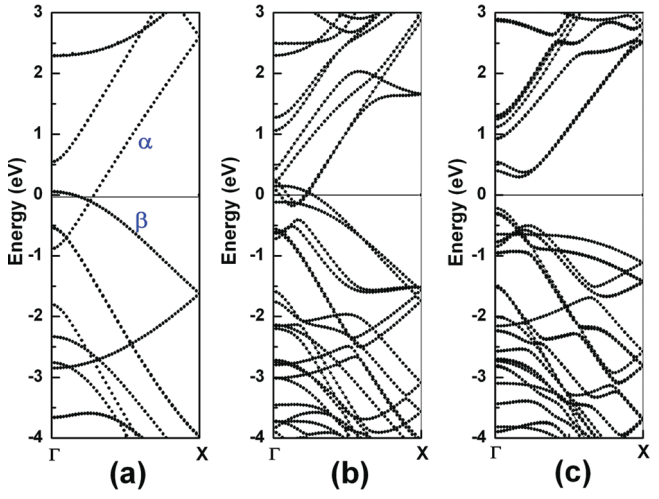

Figure 3. Calculated energy band structures of (a) freestanding (5,0) tube, (b) (5,0) doublet bundle, and (c) (5,0) triplet bundle. The Fermi level is at zero.

that the elliptic-like deformation of the (5,0) tube could lead to a metal−semiconductor transition due to the band splitting.[29] Considering that the triplet has C_3 symmetry, as a test we have calculated the band structure of just one-third of the triplet (a deformed tube). We find that the system remains metallic which suggests that the covalent bonding between the (5,0) tubes and the resulting large ratio of sp^3 carbon atoms should play a more important role in the gap opening. It is also reasonable to expect that controlling the concentration of sp^3 carbon atoms might be an effective way to manipulate the energy bands of carbon materials.

As the triplet is energetically the most favorable among all the small bundles of (5,0) tubes, we will focus on it in the following discussions. Due to its porous structure and large specific surface area, the (5,0) triplet may be at advantage in molecules adsorption and energy storage. Here we take hydrogen as an example.

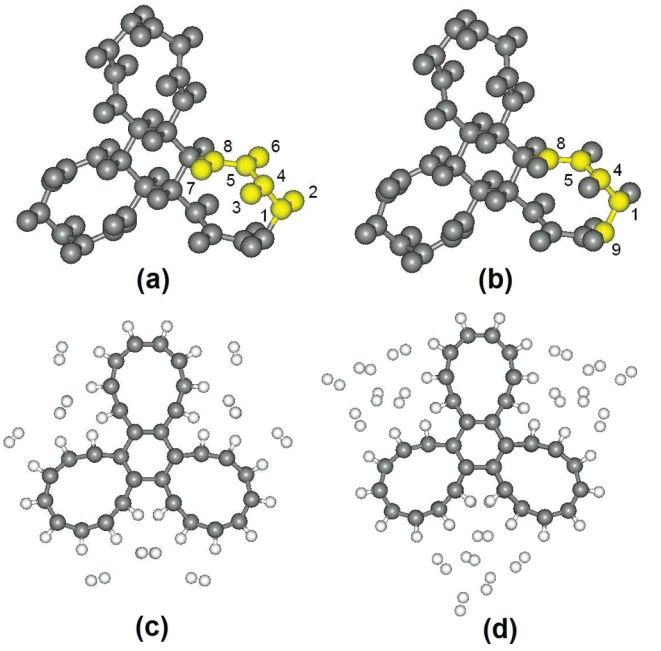

Figure 4. Possible adsorption sites for H_2 on the triplet (5,0): (a) "vertical chemisorptions", (b) "horizontal chemisorptions". (c and d) Initial and optimized configurations, respectively, for the highest hydrogen concentration with a nominal formula of $C_{60}H_{84}$.

We first consider chemisorptions of H_2 on the outer surface of the triplet. As shown in Figure 4a and 4b, there are four inequivalent adsorption sites in each blade, which are marked as 12, 34, 56, 78 for the C−C bonds along the tube axis (vertical chemisorptions), and 19, 14, 45, 58 for the C−C bonds around the tube circumference (horizontal chemisorptions). The calculated H_2 binding energies for these sites are summarized in Table 1. Here the binding energy is defined as:

$$E_b = [E(\text{triplet} + H_2) - E(\text{triplet}) - n \times E(H_2)]/n$$

dx.doi.org/10.1021/jp1120433 |J. Phys. Chem. C 2011, 115, 9227–9231

Table 1. Calculated Binding Energy and H−H Distance for H_2 Chemisorbed on Different Sites of (5,0) Triplet Marked in Figure 4a and 4b

sites	12	34	56	78
E_b	−2.42 eV	−1.69 eV	−0.73 eV	−0.81 eV
$d_{H\text{-}H}$	1.96 Å	1.99 Å	2.03 Å	2.04 Å
sites	19	14	45	58
E_b	−1.68 eV	−1.37 eV	−0.62 eV	−0.18 eV
$d_{H\text{-}H}$	2.32 Å	2.28 Å	2.16 Å	2.08 Å

where $E(\text{triplet}+H_2)$ is the total energy of the triplet with n chemisorbed H_2, $E(\text{triplet})$ is the total energy of the pristine triplet, and $E(H_2)$ is the total energy of a H_2 molecule. We see from Table 1 that all the binding energies are negative, which suggests that the chemisorptions are exothermic if the chemical potential of hydrogen is set as that of a H_2 molecule. Moreover, we find that the calculated binding energies show an interesting site dependence, with the order $E_{12} < E_{34} < E_{56} \approx E_{78}$ for the "vertical chemisorptions", and $E_{19} < E_{14} < E_{45} < E_{58}$ for the "horizontal chemisorptions". This is reasonable since the unique configuration of the triplet bundle induces an anisotropic curvature which is largest at the tip site (site 12 or 19) and smallest around the groove site (site 56, 58, or 78). The larger the curvature, the more reactive it will be. Note that the hydrogen binding energy at site 12 (−2.42 eV) is significantly lower than that of the freestanding (5,0) tube (−1.58 eV), which suggests that the triplet (5,0) is more favorable for hydrogen adsorption. On the other hand, if we compare those sites which are close to each other, we see from Table 1 that "vertical chemisorptions" always have a lower binding energy than those of "horizontal chemisorptions". This is consistent with the observation that the H−H distance of "vertical chemisorptions" is always smaller than that of "horizontal chemisorptions" and again can be attributed to the curvature effect.

It would be interesting to estimate the maximum hydrogen storage capacity of the triplet bundle. The negative numbers listed in Table 1 suggest that the hydrogen atoms can be adsorbed with a large amount. Among the 60 carbon atoms in the unit cell, there are 48 atoms with sp^2 hybridization, and all of them could be saturated by hydrogen atoms. Thus, the highest concentration of chemisorptions on the triplet is $C_{60}H_{48}$ with a binding energy of −0.46 eV/H_2. In addition, we find that the outer space of the triplet is suitable for physisorptions. In our calculations, 18 hydrogen molecules are introduced into three groove sites between adjacent tubes and are symmetrically arranged. The initial and optimized configurations are respectively shown in Figure 4(c) and Figure 4d with a nominal formula of $C_{60}H_{84}$. At this higher concentration, the calculated hydrogen binding energy is −0.32 eV/H_2, which is an average of strong chemisorptions (−0.46 eV/H_2) and relatively weak physisorptions (−0.15 eV/H_2). Among the 18 physisorbed hydrogen molecules, our additional LDA calculations find that the average binding energy is −0.17 eV/H_2 for the inner layer and −0.10 eV/H_2 for the outer layer. Both values are larger than the limiting LDA value of −0.06 eV/H_2 for the H_2 clusters.[30] This is reasonable since we are considering a different system where the triplet bundle and the chemisorbed hydrogen will enhance the binding. Moreover, our calculated results indicate that the outer layer H_2 should interact with both the inner layer H_2 and the chemisorbed triplet. All these confirm that physisorptions of those 18 hydrogen molecules are likely to occur on the groove sites. Note that our calculated binding energies for physisorptions are reasonable compared with other LDA calculations in the literature for similar systems. For example, Okamoto et al. found that the binding energy of H_2 physisorbed on graphene is −0.10 eV/H_2.[31] Arellano et al. gave a binding energy of −0.17 eV/H_2 for H_2 physisorbed inside the (5,5) carbon nanotube.[32] Ao et al. reported that for H_2 physisorbed on different sites of Al-doped graphene, the corresponding binding energy ranges from −0.136 eV/H_2 to −0.159 eV/H_2.[33] Summarizing our results, it is thus reasonable to expect that the maximum hydrogen storage capacity can be reached to $CH_{1.4}$ (or 10.4% by weight), which includes contributions from both the physisorptions (4.4 wt %) and chemisorptions (6.0 wt %). It should be noted that LDA is known to overestimate binding energies, and the standard density functional theory (DFT) calculations usually could not properly treat the long-range dispersion interactions involved in the physisorptions of H_2. Our calculated energy value thus does not mean that there is a strong interaction between the physisorbed H_2 and the triplet bundle. Instead, it should be interpreted as the upper bound for the interaction strength. We expect that more accurate treatments such as the many-body coupled cluster or Moller−Plesset perturbation method[34,35]could give an improved prediction of the binding energies. However, we believe that the basic physics reported here should not be changed. As for the desorptions, we first note that the 18 H_2 molecules physisorbed on the groove sites can be readily released. We further find from Table 1 that H_2 molecules chemisorbed on the sites 56 and 78 have smaller binding energies and may have relatively smaller desorption barriers.[36] It is thus reasonable to expect that H_2 molecules on these two sites (and those equivalent sites) can be also released by reasonable energy input. The total number of H_2 molecules that can be desorbed is thus estimated to be 30, which has a weight percentage of 7.5%. The significantly enhanced storage capacity, favorable binding energy, and relatively large desorption amount suggest that (5,0) triplet could be a very promising system for the future applications of hydrogen storage and supply.

4. SUMMARY

In summary, our density functional calculations indicate that the (5,0) tubes prefer to form small bundles by strong chemical bonds rather than the generally believed vdW interactions. The bundle state is energetically favorable and also kinetically stable. Among all the investigated (5,0) bundles, the triplet is the most favorable possibility, which shows a distinct semiconducting behavior. The unique atomic configuration gives the (5,0) triplet many unusual properties such as very large hydrogen storage capacity for practical use. Other possible applications including gas sensors and molecular motors will be the subject of our further work.

AUTHOR INFORMATION

Corresponding Author
*E-mail: phlhj@whu.edu.cn.

ACKNOWLEDGMENT

This work was supported by the Program for New Century Excellent Talents in University, the "973 Program" of China

(Grant No. 2007CB607501), and the Natural Science Foundation for the Outstanding Young Scientists of Hubei Province. We also acknowledge financial support from the interdiscipline and postgraduate programs under the "Fundamental Research Funds for the Central Universities". All the calculations were performed in the PC Cluster from Dawn Company of China.

REFERENCES

(1) Thess, A.; Lee, R.; Nikolaev, P.; Dai, H. J.; Petit, P.; Robert, J.; Xu, C. H.; Lee, Y. H.; Kim, S. G.; Rinzler, A. G.; Colbert, D. T.; Scuseria, G. E.; Tománek, D.; Fischer, J. E.; Smalley, R. E. *Science* **1996**, *273*, 483.
(2) Schlittler, R. R.; Seo, J. W.; Gimzewski, J. K.; Durkan, C.; Saifullah, M. S. M.; Welland, M. E. *Science* **2001**, *292*, 1136.
(3) Zhao, J. J.; Buldum, A.; Han, J.; Lu, J. P. *Phys. Rev. Lett.* **2000**, *85*, 1706.
(4) Dillon, A. C.; Heben, M. J. *Appl. Phys. A: Mater. Sci. Process.* **2001**, *72*, 133.
(5) Han, S. S.; Kang, J. K.; Lee, H. M.; van Duin, A. C. T.; Goddard, W. A. *Appl. Phys. Lett.* **2005**, *86*, 203108.
(6) Muniz, A. R.; Meyyappan, M.; Maroudas, D. *Appl. Phys. Lett.* **2009**, *95*, 163111.
(7) Kong, J.; Franklin, N. R.; Zhou, C. W.; Chapline, M. G.; Peng, S.; Cho, K.; Dai, H. J. *Science* **2000**, *287*, 622.
(8) Sumanasekera, G. U.; Adu, C. K. W.; Fang, S.; Eklund, P. C. *Phys. Rev. Lett.* **2000**, *85*, 1096.
(9) Zhao, J. J.; Buldum, A.; Han, J.; Lu, J. P. *Nanotechnology* **2002**, *13*, 195.
(10) Wang, Q. Y.; Challa, S. R.; Sholl, D. S.; Johnson, J. K. *Phys. Rev. Lett.* **1999**, *82*, 956.
(11) Lu, T.; Goldfield, E. M.; Gray, S. K. *J. Phys. Chem. B* **2006**, *110*, 1742.
(12) Challa, S. R.; Sholl, D. S.; Johnson, J. K. *Phys. Rev. B* **2001**, *63*, 245419.
(13) Garberoglio, G.; Johnson, J. K. *ACS Nano* **2010**, *4*, 1703.
(14) Kociak, M.; Kasumov, A. Y.; Guéron, S.; Reulet, B.; Khodos, I. I.; Gorbatov, Y. B.; Volkov, V. T.; Vaccarini, L.; Bouchiat, H. *Phys. Rev. Lett.* **2001**, *86*, 2416.
(15) Ferrier, M.; Ladieu, F.; Ocio, M.; Sacépé, B.; Vaugien, T.; Pichot, V.; Launois, P.; Bouchiat, H. *Phys. Rev. B* **2006**, *73*, 094520.
(16) Ferrier, M.; Kasumov, A. Y.; Agache, V.; Buchaillot, L.; Bonnot, A.-M.; Naud, C.; Bouchiat, V.; Deblock, R.; Kociak, M.; Kobylko, M.; Guéron, S.; Bouchiat, H. *Phys. Rev. B* **2006**, *74*, 241402(R).
(17) Bellafi, B.; Haddad, S.; Charfi-Kaddour, S. *Phys. Rev. B* **2009**, *80*, 075401.
(18) Tersoff, J.; Ruoff, R. S. *Phys. Rev. Lett.* **1994**, *73*, 676.
(19) Stahl, H.; Appenzeller, J.; Martel, R.; Avouris, Ph.; Lengeler, B. *Phys. Rev. Lett.* **2000**, *85*, 5186.
(20) López, M. J.; Rubio, A.; Alonso, J. A.; Lefrant, S.; Méténier, K.; Bonnamy, S. *Phys. Rev. Lett.* **2002**, *89*, 255501.
(21) Jiang, Y. Y.; Zhou, W.; Kim, T.; Huang, Y.; Zuo, J. M. *Phys. Rev. B* **2008**, *77*, 153405.
(22) Kleis, J.; Schröder, E.; Hyldgaard, P. *Phys. Rev. B* **2008**, *77*, 205422.
(23) Wang, N.; Tang, Z. K.; Li, G. D.; Chen, J. S. *Nature (London)* **2000**, *408*, 51.
(24) Kresse, G.; Joubert, D. *Phys. Rev. B* **1999**, *59*, 1758.
(25) Kresse, G.; Hafner, J. *Phys. Rev. B* **1993**, *47*, 558.
(26) Kresse, G.; Hafner, J. *Phys. Rev. B* **1994**, *49*, 14251.
(27) Kresse, G.; Hafner, J. *Comput. Mater. Sci.* **1996**, *6*, 15.
(28) Liu, H. J.; Chan, C. T. *Phys. Rev. B* **2002**, *66*, 115416.
(29) Connétable, D.; Rignanese, G.-M.; Charlier, J.-C.; Blase, X. *Phys. Rev. Lett.* **2005**, *94*, 015503.
(30) Martínez, J. I.; Isla, M.; Alonso, J. A. *Euro. Phys. J. D* **2007**, *43*, 61.
(31) Okamoto, Y.; Miyamoto, Y. *J. Phys. Chem. B* **2001**, *105*, 3470.
(32) Arellano, J. S.; Molina, L. M.; Rubio, A.; López, M. J.; Alonso, J. A. *J. Chem. Phys.* **2002**, *117*, 2281.
(33) Ao, Z. M.; Jiang, Q.; Zhang, R. Q.; Tan, T. T.; Li, S. *J. Appl. Phys.* **2009**, *105*, 074307.
(34) Diep, P.; Johnson, J. K. *J. Chem. Phys.* **2000**, *112*, 4465.
(35) Carmichael, M.; Chenoweth, K.; Dykstra, C. E. *J. Phys. Chem. A* **2004**, *108*, 3143.
(36) Miao, L.; Liu, H. J.; Wen, Y. W.; Zhou, X.; Hu, C. Z. *J. Appl. Phys.* **2008**, *103*, 016106.